

Chiral Porous Solids Based on Lamellar Lanthanide Phosphonates

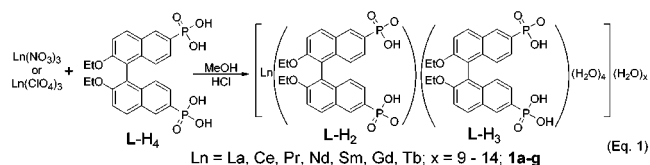
Owen R. Evans, Helen L. Ngo, and Wenbin Lin*

Department of Chemistry, CB #3290
University of North Carolina
Chapel Hill, North Carolina 27599

Received June 8, 2001

There has been tremendous recent interest in the design and synthesis of functional solids based on metal–organic coordination networks.^{1–7} In contrast to inorganic zeolites, metal–organic frameworks are typically synthesized under mild conditions and thus allow rational design of novel materials by incorporating bridging ligands with desired size, shape, chirality, and electronic properties. Over the past few years, many metal–organic coordination networks have been shown to exhibit unique properties including functional group/size selective sorption, catalysis, gas storage, molecular recognition, and second harmonic generation.^{2,6–7} With a few notable exceptions,⁶ homochiral metal–organic frameworks have not been explored for applications in heterogeneous asymmetric catalysis and enantioselective separation. Motivated by elegant work of Mallouk et al. on preparative-scale chiral separation of a racemic mixture of naphthylamines using α -Zr(HPO₄)₂ intercalated with chiral cyclophanes,⁵ we have recently explored the design and synthesis of thermally and hydrolytically robust, single-crystalline, chiral porous metal–organic frameworks based on metal bisphosphonates. Herein we wish to report the synthesis, structures, chiral separation, and catalytic properties of a series of homochiral porous lamellar lanthanide bisphosphonates.

Homochiral lanthanide bisphosphonates with the general formula of [Ln(L-H₂)(L-H₃)(H₂O)₄] \cdot xH₂O (Ln = La, Ce, Pr, Nd, Sm, Gd, Tb, x = 9–14, **1a–g**) were synthesized by slow evaporation of an acidic mixture of nitrate or perchlorate salts of Ln(III) and 2,2'-diethoxy-1,1'-binaphthalene-6,6'-bisphosphonic acid(L-H₄)⁸ in methanol at room temperature (eq 1). The IR



spectra of **1a–g** display strong phosphorus–oxygen stretches at 950–1150 cm⁻¹. In addition, the IR spectra of **1a–g** also exhibit

(1) (a) Desiraju, G. R. *Crystal Engineering: The Design of Organic Solids*; Elsevier: New York, 1989. (b) Lehn, J.-M. *Supramolecular Chemistry: Concepts and Perspectives*; VCH Publishers: New York, 1995. (c) Batten, S. R.; Robson, R. *Angew. Chem., Int. Ed.* **1998**, *37*, 1461. (d) Zawarotko, M. J. *Chem. Soc. Rev.* **1994**, 283.

(2) (a) Fujita, M.; Kwon, Y. J.; Washizu, S.; Ogura, K. *J. Am. Chem. Soc.* **1994**, *116*, 1151. (b) Eddaoudi, H. L.; O'Keeffe, M.; Yaghi, O. M. *Nature* **1999**, *402*, 276. (c) Gardner, G. B.; Kiang, Y. H.; Lee, S.; Asgaonkar, A.; Venkataraman, D. *J. Am. Chem. Soc.* **1996**, *118*, 6946. (d) Kiang, Y. H.; Gardner, G. B.; Lee, S.; Xu, Z. T.; Lobkovsky, E. B. *J. Am. Chem. Soc.* **1999**, *121*, 8204.

(3) (a) Clearfield, A. *Prog. Inorg. Chem.* **1998**, *47*, 371. (b) Clearfield, A. *Chem. Mater.* **1998**, *10*, 2801. (c) Alberti, G. *Comprehensive Supramolecular Chemistry*; Pergamon Press: New York, 1996; Vol. 7, pp 151–185. (d) Cao, G.; Lynch, V. M.; Swinnea, J. S.; Mallouk, T. E. *Inorg. Chem.* **1990**, *29*, 2112.

(4) (a) Mallouk, T. E.; Gavin, J. A. *Acc. Chem. Res.* **1998**, *31*, 209. (b) Zhang, Y.; Frink, K. J.; Clearfield, A. *Chem. Mater.* **1993**, *5*, 495. (c) Frink, K. J.; Wang, R.-C.; Colon, J. L.; Clearfield, A. *Inorg. Chem.* **1991**, *30*, 1438. (d) Johnson, J. W.; Jacobsen, A. J.; Butler, W. M.; Rosenthal, S. E.; Brady, J. F.; Lewandowski, J. T. *J. Am. Chem. Soc.* **1989**, *111*, 381.

(5) Garcia, M. E.; Naffin, J. L.; Deng, N.; Mallouk, T. E. *Chem. Mater.* **1995**, *7*, 1968.

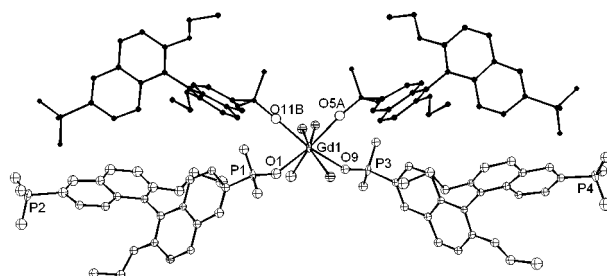


Figure 1. Coordination environment of **1f**. The asymmetric unit (excluding water guest molecules) is shown with ellipsoids at 30% probability.

intense and broad O–H stretching vibrations between 3700 and 3200 cm⁻¹. Thermogravimetric analyses show that **1a–g** lose 11.7–17.4% of total weight by 90 °C, corresponding to the loss of 9–14 water molecules per formula unit (expected 11.6–17.2%).⁹ These formulations have been supported by microanalysis results (Supporting Information).

A single-crystal X-ray diffraction study performed on [Gd(R-L-H₂)(R-L-H₃)(H₂O)₄] \cdot 12H₂O (**R-1f**) reveals a 2D lamellar structure consisting of 8-coordinate Gd centers and bridging binaphthylbisphosphonate groups. **1f** crystallizes in the chiral space group *P*₂₁₂₁.¹⁰ The asymmetric unit of **1f** consists of one Gd center, two bridging binaphthylbisphosphonate groups, four coordinated water molecules and 12 water guest molecules (Figure 1). The Gd center adopts a square anti-prismatic geometry by coordinating to four water molecules and four phosphonate oxygen atoms of four different binaphthylbisphosphonate ligands. Three of the four crystallographically independent phosphonate groups (P1–P3) are monodeprotonated and coordinate to the Gd center in a monodentate fashion, while the fourth phosphonate group (P4) remains protonated and also coordinates to the Gd center in a monodentate fashion.¹¹ If we disregard the coordinated water molecules, the four phosphonate groups coordinate to the Gd center in a highly distorted tetrahedral geometry with O–Gd–O angles ranging from 81.4 to 147.4°. The binaphthyl subunits have dihedral angles of 118.2 and 121.0° for L-H₂ and L-H₃, respectively. The skewed configuration of the binaphthyl subunits in combination with the distorted tetrahedral phosphonate coordination allows the formation of an elongated 2D rhombohedral grid lying in the *ac* plane (Figure 2a). The 2D grid has Gd–Gd–Gd angles of 153.6 and 26.7°, and Gd–Gd separations of 16.83 and 16.78 Å. Such 2D

(6) ¹H NMR spectra of a digested mixture of Na₂(EDTA) and **1a** in D₂O show the absence of peaks characteristic of methanol, indicating that the volatile guest species in **1a–g** are water molecules.

(7) (a) Seo, J. S.; Whang, D.; Lee, H.; Jun, S. I.; Oh, J.; Jeon, Y. J.; Kim, K. *Nature* **2000**, *404*, 982. (b) Kepert, C. J.; Prior, T. J.; Rosseinsky, M. J. *J. Am. Chem. Soc.* **2000**, *122*, 5158.

(8) (a) Lin, W.; Evans, O. R.; Xiong, R.-G.; Wang, Z. *J. Am. Chem. Soc.* **1998**, *120*, 13272. (b) Lin, W.; Wang, Z.; Ma, L. *J. Am. Chem. Soc.* **1999**, *121*, 11249. (c) Evans, O. R.; Xiong, R.-G.; Wang, Z.; Wong, G. K.; Lin, W. *Angew. Chem., Int. Ed.* **1999**, *38*, 536. (d) Lin, W.; Ma, L.; Evans, O. R. *Chem. Commun.* **2000**, 2263. (e) Evans, O. R.; Lin, W. *Chem. Mater.* **2001**, *13*, 2705.

(9) L-H₄ was synthesized via a Pd-catalyzed phosphonation reaction between 6,6'-dibromo-2,2'-diethoxy-1,1'-binaphthalene and diethyl phosphite. See: (a) Jaffrès, P.-A.; Bar, N.; Villemain, D. *J. Chem. Soc., Perkin Trans. 1* **1998**, 2083. (b) Hirao, T.; Masunaga, T.; Ohshiro, Y.; Agawa, T. *Synthesis* **1981**, 56.

(10) X-ray single-crystal diffraction data for **1f** was collected on a Bruker SMART CCD diffractometer. Crystal data for **1f**: orthorhombic, space group *P*₂₁₂₁, with *a* = 7.771(1) Å, *b* = 23.900(2) Å, and *c* = 32.676(2) Å, *V* = 6068.8(6) Å³, *Z* = 4, *D*_{calc} = 1.63 g/cm³, *T* = 213 K, Mo K α radiation (λ = 0.71073 Å). Least-squares refinement based on 8025 reflections with *I* > 2 σ (*I*) and 708 parameters led to convergence, with a final value of *R*₁ = 0.097 and *wR*₂ = 0.188. (b) Lin, W.; Ma, L.; Evans, O. R. *Chem. Commun.* **2000**, 2263.

(11) The P–O distances about P4 are consistent with this formulation. The P4–O11 distance is 1.47 Å, whereas the P–OH distances are 1.54 and 1.55 Å, respectively.

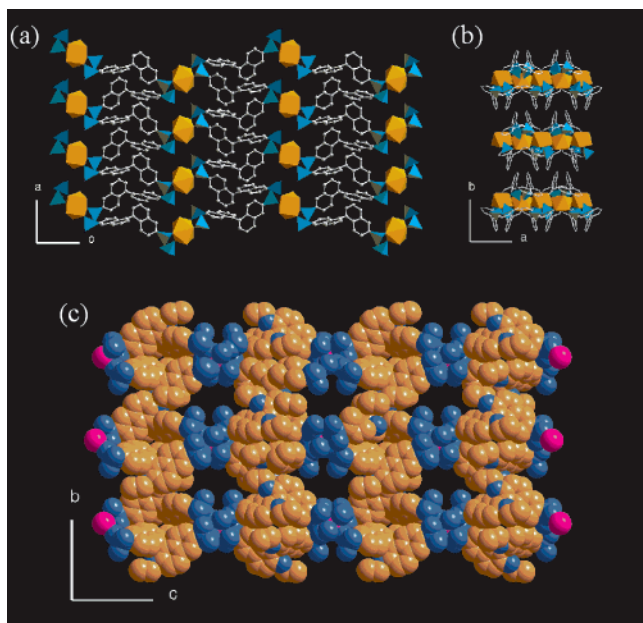


Figure 2. (a) A view of 2D framework of **1f** down the *b* axis. Ethoxy groups have been omitted for clarity. (b) A view of stacking of 2D framework of **1f** along the *c* axis showing interdigitation of binaphthyl rings from adjacent layers. The coordination environments of P atoms and Gd atoms are represented with blue and orange polyhedra, respectively. (c) A space-filling model of **1f** viewed down the *a* axis.

grids stack along the *b* axis via interdigitation of the binaphthyl rings from the adjacent layers (Figure 2b). There is still void space formed between the lamellae after such interdigitation of the binaphthyl rings, and a space-filling model of **1f** viewed along the *a* axis clearly indicates the presence of large asymmetric channels with a largest dimension of ~ 12 Å. X-ray powder diffraction studies indicate that **1a–g** are isomorphous, while CD spectra show that **1e** samples made from *R*- and *S*-L-H₄ are supramolecular enantiomers (Supporting Information).

We have studied the framework stability of **1a–g** using powder X-ray diffraction techniques. Upon evacuation at room temperature and 10^{-2} Torr for 24 h, compounds **1a–g** experienced weight losses consistent with the removal of 9–14 water molecules per formula unit. While the major peaks in the XRPD patterns of desolvated **1a–g** have broadened significantly, XRPD patterns identical to those of the pristine samples were obtained upon exposing desolvated **1a–g** to water vapor (Figure 3). Such behavior is consistent with a distortion of the long-range lamellar-type structure with preservation of local coordination environments of **1a–g** during desolvation.

Good framework stability and reversibility of the dehydration processes of **1a–g** have prompted us to explore their applications in heterogeneous catalysis and chiral separation. The presence of both Lewis and Brønsted acid sites in **1a–g** has rendered them capable of catalyzing several organic transformations including cyanosilylation of aldehydes and ring opening of *meso*-carboxylic anhydrides. Treatment of benzaldehyde (1 mmol) and cyanotrimethylsilane (2 mmol) with a CH₂Cl₂ (5 mL) suspension of powdered and desolvated **1e** (0.1 mmol) afforded mandelonitrile in 69% yield after acidic workup. Similar reactions with 1-naphthaldehyde and propionaldehyde afforded the corresponding cyanohydrin products in 55 and 61% yield, respectively. The indiscriminate catalytic efficiency between aldehydes with varying sizes suggests that the lamellar lanthanide phosphonates can readily swell to facilitate substrate transport under reaction

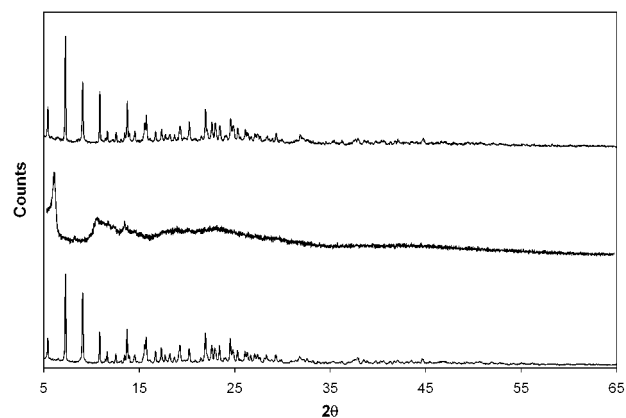


Figure 3. XRPD for **1e** before removal of water guest molecules (top), after removal of water guest molecules (middle), and upon subsequent exposure to water vapor (bottom).

conditions. In all three cases, the products were essentially racemic (*ee* < 5%).¹² We have also examined the use of **1e** in the Lewis-acid promoted ring opening of *meso*-anhydrides. Treatment of *meso*-2,3-dimethylsuccinic anhydride (1 mmol) with methanol (10 mmol) in a dry THF (5 mL) suspension of powdered and desolvated **1e** (0.1 mmol) afforded the corresponding hemiester in 81% yield with a disappointingly low *ee* of <5%.¹³ Both cyanosilylation and ring-opening reactions are apparently catalyzed heterogeneously since no reaction took place with the supernatant obtained from a suspension of **1e**.¹⁴ Moreover, ³¹P NMR spectroscopy shows that these supernatants are free from ligand contamination. Upon completion of all reactions, the catalysts could be recovered in quantitative yields (>98%) and used repeatedly without the loss of catalytic activity.

A preliminary attempt of enantioselective separation of racemic *trans*-1,2-diaminocyclohexane with ammonia-treated *R*-**1e** at a substrate/host ratio of 1.4 gives an enantio-enrichment of 13.6% in *S,S*-1,2-diaminocyclohexane in the beginning fractions and an enantio-enrichment of 10.0% in *R,R*-1,2-diaminocyclohexane in the ending fractions.¹⁵ Despite the limited enantioselectivity, **1a–g** represent a new generation of robust recyclable chiral porous solids that are capable of chiral separation and heterogeneous catalysis. With a precise knowledge of their single crystal structures and facile tunability of their building blocks, the present research holds great promise in the development of novel chiral porous materials capable of separation and catalysis with practically useful enantioselectivity.

Acknowledgment. We acknowledge NSF (CHE-9875544) for financial support. We also thank Dr. Richard Staples at Harvard University for X-ray data collection. W.L. is an Alfred P. Sloan Fellow, an Arnold and Mabel Beckman Young Investigator, and a Cottrell Scholar of Research Corp.

Supporting Information Available: Experimental procedures, analytical data, five figures, and one table (PDF). An X-ray crystallographic file (CIF). This material is available free of charge via the Internet at <http://pubs.acs.org>.

JA0163772

(12) The enantiomeric excesses of the products were determined from ¹H NMR analysis on the (+)- α -methoxy- α -trifluoromethylphenylacetic acid [(+)-MTPA] esters of the cyanohydrins.

(13) The *ee* was assessed from the ¹H NMR analysis of the amide formed from the reaction of the hemiester with (*R*)-(+)-1-(1-naphthyl)ethylamine in the presence of thionyl chloride.

(14) **1e** also efficiently catalyzed Diels–Alder reaction between methyl acrylate and cyclopentadiene.

(15) The *ee* was determined by chiral HPLC analysis after derivatization with *m*-toluoyl chloride.